Letter

Antiferro octupolar order in the $5d^1$ double perovskite Sr_2MgReO_6 and its spectroscopic signatures

Dario Fiore Mosca [1] and Leonid V. Pourovskii [2,3]

[1] *University of Vienna, Faculty of Physics and Center for Computational Materials Science, Kolingasse 14-16, 1090 Vienna, Austria*
[2] *CPHT, CNRS, École polytechnique, Institut Polytechnique de Paris, 91120 Palaiseau, France*
[3] *Collège de France, Université PSL, 11 place Marcelin Berthelot, 75005 Paris, France*

(Received 31 March 2025; accepted 24 June 2025; published 15 July 2025)

"Hidden"-order phases with high-rank multipolar order parameters have been recently detected in several cubic double perovskites of 5*d* transition metals. Here, by constructing and solving an *ab initio* low-energy Hamiltonian, we show that an antiferroic order of magnetic octupoles also forms in the tetragonal $5d^1$ double perovskite Sr_2MgReO_6. The low-temperature order in this material is determined by a tetragonal crystal field dominating over exchange interactions. This results in a well isolated crystal-field doublet ground state hosting octupolar low-energy degrees of freedom. Very weak dipole moments entangled with the primary octupole order parameters are induced by admixture of the excited $j1/2$ spin-orbit multiplet. We show that the octupolar order leads to characteristic quasigapless magnetic excitation spectra, as well as to the intensity of superstructural neutron diffraction reflexes peaking at large scattering momenta.

DOI: 10.1103/tvp5-mpy9

Introduction. The importance of the relativistic spin orbit (SO) coupling extends across different areas of chemistry and physics. Its effect of entangling spin and orbital degrees of freedom is especially important for the case of correlated insulators, where it is predicted to foster a variety of unconventional and exotic states of matter [1–4]. The family of heavy transition metal oxides falls in this category and it has attracted much interest because of the possibility of realizing exotic low-temperature phases like the elusive Kitaev spin liquid in $5d^5$ Mott insulators [5,6], or high-rank multipole orders. The latter, which are challenging to detect with conventional experimental probes and thus referred to as hidden, have been reported [7–9] in d^1 and d^2 double perovskites (DPs) $A_2BB'O_6$ (where B' is a heavy magnetic transition metal ion, A and B are nonmagnetic cations).

An intensive experimental and theoretical effort has recently been focused on the $5d^1$ DPs where the unquenched orbital angular momentum ($l = 1$) produced by the octahedral crystal field (CF) of ligands is coupled through SO to the spin ($S = 1/2$). This SO entanglement results in a total angular momentum $j_{\rm eff} = 3/2$ ground state multiplet (GSM) [See Fig. 1(a)], which can host high rank multipoles [3]. Initially, theoretical studies primarily focused on electronic exchange and electrostatic interactions [10–12], suggesting that these mechanisms could drive the ordering of charge quadrupoles without breaking time-reversal symmetry, and subsequently induce a paramagnetic to canted antiferromagnetic (cAFM) phase transition. Experimental investigations of cubic $5d^1$ DPs such as Ba_2MgReO_6 [9,13] and Ba_2NaOsO_6 [8], have confirmed the existence of this two-step phase transition. However, the origin is now largely attributed to either vibronic interactions within the $j_{\rm eff} = 3/2$ GSM, which are Jahn-Teller active [14–16], or to their interplay with electronic superexchange interactions [17–19]. While cubic DPs (space group $Fm\bar{3}m$) have attracted considerable interest, other structural variants have been relatively overlooked, despite their potential to host intriguing unconventional orders. Notably, Chen and coworkers [10] pointed out the possibility of an antiferroic ordering of magnetic octupoles with a "vanishing static magnetic dipole moment" for tetragonal DPs with elongated $B'O_6$ octahedra (or easy-axis anisotropy). The spin-orbit DPs that exhibit an elongation of the octahedra are, to our knowledge, the following: Sr_2MgReO_6 (SMRO), Sr_2CaReO_6, Sr_2ZnReO_6, and Sr_2LiOsO_6 [20–24]. Of these four, the ones that keep a tetragonal space group symmetry I4/m down to low temperatures are Sr_2LiOsO_6 [22] and SMRO [21]. However, both compounds exhibit, concomitantly with the octahedra elongation, an in-plane tilt [see Fig. 1(b)] that was initially suggested to possibly hinder the formation of octupolar phases [10]. In this study, we will focus on SMRO due to a broader range of experimental data available, as will be detailed in the following.

Initial studies on powder samples proposed SMRO to be a spin glass, as inferred from the absence of magnetic reflections in their neutron diffraction experiment, a broad peak in the magnetic susceptibility at ∼50 K accompanied by a weak bump in the heat capacity and a bifurcated magnetic susceptibility in field cooling and zero-field cooling measurements up to 300 K [20]. In a recent work, Gao and coworkers [25] were able to synthesize a single crystal of SMRO and characterize it with synchrotron x-ray diffraction, heat capacity, and magnetic susceptibility measurements. Their finding is a single second-order phase transition at $T_N \sim 50$ K toward a collinear dipolar antiferromagnetic (AFM) order with $\mathbf{q} =$

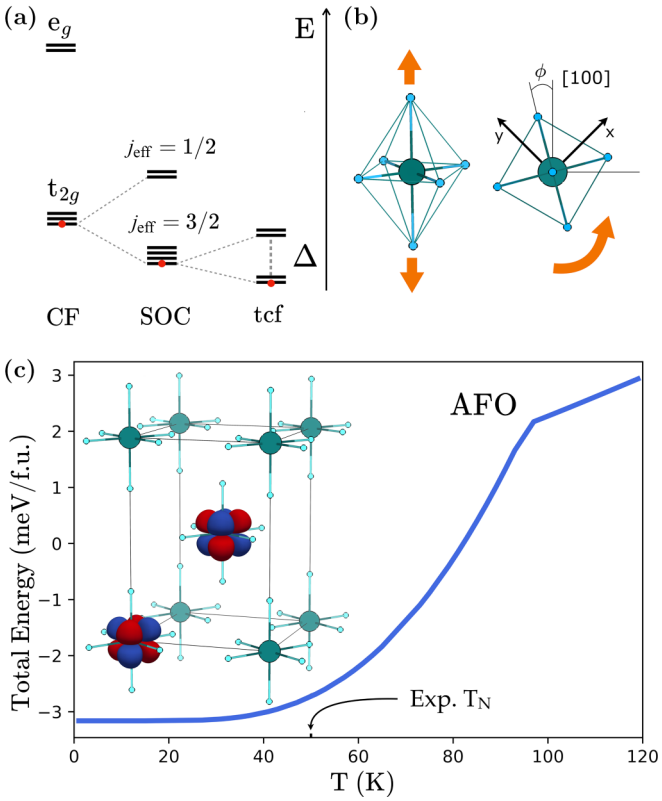

FIG. 1. (a) The electronic energy levels of $5d^1$ DPs in presence of cubic CF, SOC, and tcf. Δ is the $j_{\rm eff} = 3/2$ tcf energy splitting. (b) The octahedral distortions present in SMRO: elongation (left) and tilting (right). The angle of tilting ϕ is defined with respect to the [100] cubic crystallographic axis, rotated by 45° in our unit cell with respect to the global reference frame. (c) Mean-field ordering energy vs temperature calculated from Eq. (1) for the room temperature structure with $\delta = c/(\sqrt{2}a) - 1 = 6.6 \times 10^{-3}$. The inset shows the antiferro octupolar ordering of $O^3_{\Gamma_{5,y}}$ alone for clarity.

(001). The Re L_3 edge x-ray absorption spectrum at ∼6 K allowed the authors to infer that the magnetic moments lie within the *ab* plane, but both the crystallographic direction and the magnitude of the ordered magnetic moments are yet to be resolved [25].

In this Letter, we investigate the magnetic phase of SMRO using advanced first-principles calculations, uncovering a hidden antiferro $\mathbf{q} = (001)$ order of magnetic octupoles (AFO). The formation of the AFO order is induced by a strong tetragonal crystal-field splitting of the $j_{\rm eff} = 3/2$ ground state leading to a well-isolated GS doublet hosting planar octupolar moments. We fully characterize the AFO ordering, analyzing the role of the tetragonal crystal field and the in-plane tilting of the octahedra in its stabilization. Our calculations also predict that mixing between the $j_{\rm eff} = 3/2$ states and excited SO $j_{\rm eff} = 1/2$ doublet induces weak dipolar moments entangled with the leading octupolar order parameters. Furthermore, we identify unambiguous signatures of the AFO order in elastic and inelastic neutron scattering. The AFO order is predicted, in contrast to a conventional $\mathbf{q} = (001)$ dipole order, to feature weak superstructural Bragg peaks with intensity peaked at large *Q*-vectors and a quasigapless magnetic excitation spectrum.

Effective Hamiltonian. The structure of SMRO exhibits tetragonal symmetry at room temperature. As a result, the tetragonal crystal field (tcf) lifts the degeneracy of the $j_{\rm eff} = 3/2$ GSM promoting the $m_j = \pm 3/2$ ($m_J = \pm 1/2$) states if an elongation (compression) of the unit cell appears [see Fig. 1(a)]. While recent experimental and theoretical results propose that vibronic interactions remain active despite the noncubic symmetry of the system [26], it is questionable whether they play a role in the magnetic properties.

The many-body effective Hamiltonian employed for our study of SMRO incorporates both the electron-mediated intersite exchange interactions (IEI) and the tcf term. The IEI Hamiltonian, which describes the interactions between multipolar moments with a defined total angular momentum $j_{\rm eff} = 3/2$, is expressed within the framework of this effective Hamiltonian, as

$$H_{\rm eff} = \sum_{\langle ij \rangle} \sum_{\substack{KK' \\ \Gamma,\gamma,\Gamma',\gamma'}} V^{KK'}_{\Gamma\Gamma',\gamma\gamma'}(ij) O^K_{\Gamma\gamma}(i) O^{K'}_{\Gamma'\gamma'}(j) + \sum_i H^i_{\rm tcf}, \tag{1}$$

where the first summation (ij) runs over the Re-Re bonds, the second summation over the multipolar momenta of the ranks $K, K' = 1, 2, 3$, and irreducible representation (IREP) Γ with projections γ. $O^K_{\Gamma\gamma}(i)$ are the normalized multipolar operators of the rank *K*, IREP Γ, and projection γ acting on the Re site *i* [3,27]. $V^{KK'}_{\Gamma\Gamma',\gamma\gamma'}(ij)$ represents the corresponding IEI. We explicitly include the tcf term $H^i_{\rm tcf} = V_{\rm tcf} O^2_{\Gamma_3,z^2}(i)$.

Methods. We first calculate the paramagnetic electronic structure of SMRO using the charge self-consistent density functional theory (DFT) [28] + dynamical mean-field theory [29–32] within the quasiatomic Hubbard-I (HI) approximation [33]. We then determine the multipolar IEI in Eq. (1) using the force theorem in the Hubbard-I (FT-HI) approach of Ref. [34]. We employ the FT-HI implementation provided by the publicly available MagInt code, which enables IEI computation for general lattice structures containing multiple correlated sites [35]. See Supplemental Material (SM) [36] for further details.

We use the tetragonally distorted room temperature structure of SMRO from Ref. [25] with $a = 5.578$ Å, $c = 7.941$ Å. Our DFT + HI calculations correctly reproduce the Re^{6+} ground state multiplet $j_{\rm eff} = 3/2$, with tcf splitting $\Delta \approx 28$ meV [see also Fig. 1(a)]. The SO splitting between $j_{\rm eff} = 3/2$ and $j_{\rm eff} = 1/2$ states is ≈0.48 eV, in good agreement with the experimental value of 0.53 eV from Ref. [26], and the $t_{2g} - e_g$ CF splitting is ≈4.6 eV. Following the previous works [17], and in contrast to other proposed approaches for multipolar orders in spin-orbit Mott insulators [37,38], we restrict the IEIs to the $j_{\rm eff} = 3/2$ manifold. This is justified by the fact that the strongest calculated $V^{KK'}_{\Gamma\Gamma',\gamma\gamma'}(ij)$ (listed in the SM [36]) is of about 4 meV ≪ SOC splitting. The largest IEI values are also considerably smaller than Δ, implying that the ordered phase will be governed by the IEI acting within the ground-state doublet $m_j = \pm 3/2$.

This low-lying GSM can therefore be encoded by spin-1/2 operators τ_α, with the states corresponding to the projections of pseudo-spin-1/2. The resulting pseudospin Hamiltonian,

$$H = \sum_{\langle ij \rangle} \sum_{\alpha\beta} J_{\alpha\beta}(ij) \tau_\alpha(i) \tau_\beta(j), \tag{2}$$

TABLE I. Calculated IEI downfolded into the $m_J = \pm 3/2$ manifold for the in-plane and out-of-plane Re-Re bonds (in meV).

	R = [0.5, 0.5, 0]				**R** = [0.5, 0, 0.5]		
	x	y	z		x	y	z
x	0.55	0	0	x	4.48	0	0.05
y	0	0.55	0	y	0	4.51	−0.09
z	0	0	0.45	z	0.05	−0.09	2.73

is Eq. (1) downfolded into the $m_J = \pm 3/2$ space. Up to a normalization factor, τ_x is a combination of $O^3_{\Gamma_4,x}$ and $O^3_{\Gamma_5,x}$, τ_y is a combination of $O^3_{\Gamma_4,y}$ and $O^3_{\Gamma_5,y}$, and τ_z is a combination of $O^3_{\Gamma_4,z}$ and dipole $O^1_{\Gamma_4,z}$ (see the SM for the derivation of the reduced Hamiltonian [36]). Overall, the ordering within this low-energy τ space arises from the competition between purely octupolar operators (τ_x, τ_y) and the mixed dipole-octupole τ_z. The final IEI pseudospin matrix for lattice vectors in the *ab* plane ([1/2,1/2,0]) and *ac* plane ([1/2,0, 1/2]) are given in Table I.

We find that the interactions within the *ab* plane are an order of magnitude weaker than those in the *ac* and *bc* planes. This is a consequence of the positive single ion anisotropy induced by the tcf, which promotes *xz* and *yz* orbital occupations. The strongest interactions are J_{xx} and J_{yy}, which are identical in the *ab* plane and differ only slightly for the out-of-plane bonds. Their positive signs indicate an antiferromagnetic coupling between $O^3_{\Gamma_4,x}, O^3_{\Gamma_5,x}$ and $O^3_{\Gamma_4,y}, O^3_{\Gamma_5,y}$ octupoles, respectively. The interaction matrices are seen to almost exactly obey the U(1) symmetry as expected at the large tcf limit [10].

Ordered phase. Next, we solve the full multipolar Hamiltonian of Eq. (1) within a single-site mean field (MF) using the "McPhase" package [39] together with an in-house module. Care should be exercised in evaluating the realistic magnetic moment of the SMRO $j_{\text{eff}} = 3/2$ shell. The quasiatomic approximation leads to the gyromagnetic factor $g_J = 0$ due to a perfect cancellation of its spin and orbital moments. This cancellation does not occur in real SMRO, which exhibits the effective Curie-Weiss moment of $0.8\,\mu_B/f.u.$ corresponding to $g_J = 0.413$ [25]. The nonzero magnetic moments of d^1 DPs can be explained by covalency of $5d$-O-p bonds reducing the $5d$ orbital magnetization [40,41]. We note that our DFT + HI framework includes, in principle, this covalency effect through admixture of ligand-p character to $5d$ Wannier orbitals that we construct from a "narrow" energy window enclosing $5d$ bands [32,36,42]. However, calculating the orbital magnetic moment for such extended Wannier orbitals is a rather complex procedure [41], which is outside of the scope of this work focused on effective magnetic Hamiltonians and order parameters. Correspondingly, we treat this effect in a semiempirical way by employing the experimental g_J value, which corresponds to the covalency factor $\gamma = 1 - 3g_J/2 = 0.38$, to compute MF magnetic moments.

We find that SMRO undergoes a single second-order phase transition at temperature $T_N \approx 92$ K into an AFO order with the propagation wave vector $\mathbf{q} = [0, 0, 1]$ and an octupolar order parameter (OP) that is a mixture of four octupoles [see Fig. 1(c)]. These octupole moments have the following magnitudes: $\langle O^3_{\Gamma_4,y}\rangle \approx 0.54$, $\langle O^3_{\Gamma_5,y}\rangle \approx 0.42$, $\langle O^3_{\Gamma_4,x}\rangle \approx -0.16$, and $\langle O^3_{\Gamma_5,x}\rangle \approx 0.13$. Due to the neglect of local fluctuations and short-range correlations in the MF approximation, the calculated Néel temperature is overestimated by ∼46%, consistent with previous applications of the present framework [43–45]. Moreover, our results indicate that this AFO order is hidden behind a collinear AFM phase composed of weak dipolar magnetic moments (∼$0.06\,\mu_B$) with the same wave vector and oriented within the *ab* plane with an angle of ∼25° relative to the *x* global axis of Fig. 1(b).

The dipoles in the AFM phase are not the primary order parameters. They arise directly from the octupolar order for the following reasons: (i) We find the MF dipole moments to be negligible in magnitude compared to the octupole ones. This comparison is meaningful because the operators $O^K_{\Gamma\gamma}$ are uniformly normalized. Therefore, the expectation values of moments of different rank can be directly compared to evaluate their degree of saturation. (ii) When computing the magnetic moments M_α with $\alpha = x, y, z$ hosted by the Re $5d$ shell in the saturated $j_{\text{eff}} = 3/2$ AFO order with the covalency factor $\gamma = 1$, we find a maximum in-plane moment of $0.16\,\mu_B$, with increasing values as the tcf increases (see the SM [36] for details).

This seemingly paradoxical result (pure octupoles do not carry a dipole moment) is explained by mixing of the GSM $j_{\text{eff}} = 3/2$ with $j_{\text{eff}} = 1/2$ states due to the tcf. As a result, the octupoles defined within the $j_{\text{eff}} = 3/2$ space acquire a small admixture of dipole character upon mapping into physically observable moments of the $5d$ shell. The increase in magnetic moment with increasing tcf further supports this interpretation.

Tilting vs elongation. Early measurements on SMRO and similar systems revealed the emergence of a "glassy state," suggesting that either the tcf was not strong enough to stabilize the octupolar-active GSM or that octahedral tilting played a role in suppressing the AFO phase [10]. To examine this effect, we conducted a series of calculations, systematically varying the tcf through $\delta = c/(\sqrt{2}a) - 1$ and the tilting angle ϕ [see Fig. 1(b)], while keeping the volume and in-plane Re–O bondlength fixed. The volume constraint is justified by the minimal shrinkage observed across the temperature range (∼0.4% [25]), while the fixed in-plane bondlength aligns with experimental findings, which show a significant change in the Re–O(z) bond length while the in-plane bond lengths remain largely unaffected [25].

Our results, summarized in the phase diagram of Fig. 2, reveal a region of dipolar cAFM order, which persists until the tcf produced by the octahedral elongation or tilting angle induce an energy splitting of $\Delta \sim 8$ meV; i.e., when the IEI mean exchange field becomes comparable to the splitting of the $j_{\text{eff}} = 3/2$ states. Beyond this threshold, AFO order dominates. For comparison, the fading thick line in Fig. 2 traces the experimentally observed evolution of the structural parameters. While the exact location of the cAFM-AFO boundary may be sensitive to the DFT + HI parameters, our calculations with different U values show that SMRO always lies within the AFO region at all temperatures (see the SM [36]). Interestingly, the tilting behaves effectively as a tcf with a quasi-exponential scaling at small ϕ, thus promoting the AFO phase, rather than suppressing it (see the SM [36]).

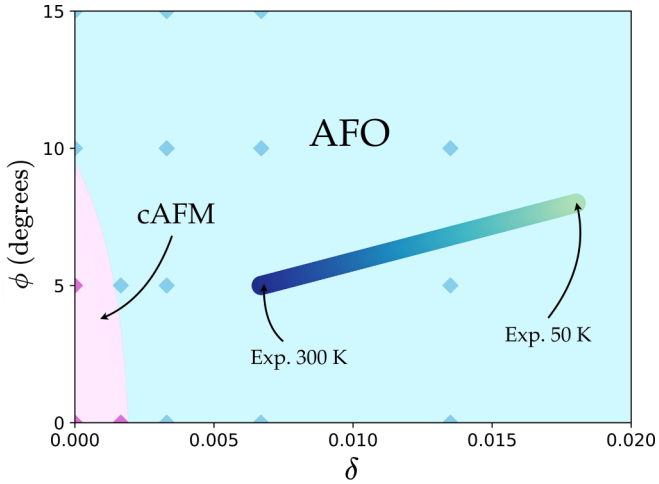

FIG. 2. Phase diagram of SMRO as a function of $\delta = c/(\sqrt{2}a) - 1$ and ϕ (tilting angle). The diamond data-points refer to the actual DFT + HI calculations, while the the fading thick line is the "path" in the phase diagram of the SMRO structure as a function of temperature. The Re-O in-plane bondlength has been kept fixed as found experimentally [25].

Neutron scattering. In order to identify experimental signatures of the predicted octupolar order, we have calculated elastic and inelastic neutron scattering in the AFO phase. For the sake of comparison, we have also calculated the same quantities for the hypothetical cAFM phase, which is predicted, as discussed above, to be realized in cubic SMRO.

First, we focus on the magnetic elastic Bragg scattering at the superstructural positions $\mathbf{G} = 2\pi[h/a, k/a, l/c]$, where a and c are the lattice parameters, with $h + k + l = 2n + 1$ that are forbidden in the $I4/m$ space group of SMRO. The magnetic Bragg peak intensity reads

$$|F(\mathbf{G})|^2 = \sum_{\alpha\beta}(\delta_{\alpha\beta} - \hat{G}_\alpha \hat{G}_\beta) F_\alpha(\mathbf{G}) F^*_\beta(\mathbf{G}),$$

where $F_\alpha(\mathbf{G}) = \sum_{\mathbf{R}KQ} F^\alpha_{KQ}(\mathbf{G}) \langle O^K_Q \rangle_{\mathbf{R}} \exp(i\mathbf{GR})$ is the structure factor, $\hat{\mathbf{G}} = \mathbf{G}/|G|$, and $\alpha, \beta = x, y, z$ [46]. In the structure factor, $\langle O^K_Q \rangle_{\mathbf{R}}$ is the multipolar order parameter on the sublattice $\mathbf{R}$ in a given ordered phase, and $F^\alpha_{KQ}(\mathbf{G})$ is the corresponding neutron scattering form factor. In order to include the contribution to scattering from octupoles, we calculate the form factors beyond the dipole approximation for all magnetic multipoles KQ using the approach of Refs. [45,47]. This method employs the expressions of Ref. [48] to evaluate one-electron matrix elements of the spin $\hat{\mathbf{Q}}_s$ and orbital $\hat{\mathbf{Q}}_o$ neutron scattering operators for the $5d$ shell. The resulting matrices are then projected into the $j_{\text{eff}} = 3/2$ space and expanded in multipole operators as in the previous application of this method to d^2 DP of Os [45]. To approximately include the effect of covalency on the form factors, we scale down the contribution due to $\hat{\mathbf{Q}}_o$ in the neutron-scattering matrix elements with the experimental covalency factor γ.

The calculated intensities of superstructural peaks are then "powder averaged" as $\sum_{\{G\}} |F(\mathbf{G})|^2/G^2$, where the sum is over all $\mathbf{G}$ belonging to a given star, to simulate polycrystalline SMRO. The resulting intensities in the AFO phase [Fig. 3(a)] peak at large $\mathbf{G}$ vectors with the largest magnitude obtained for the $\langle 131 \rangle$ reflection corresponding to $G = 3.65\,\text{Å}^{-1}$. In contrast, the cAFM intensities exhibit a rapid decay vs G that is typical for magnetic reflections. This remarkable qualitative distinction between the two phases stems from different behavior of dipole and octupole form factors, with the former peaked at $G \to 0$, while the latter reaching maximum magnitudes at finite G of several Å^{-1}.

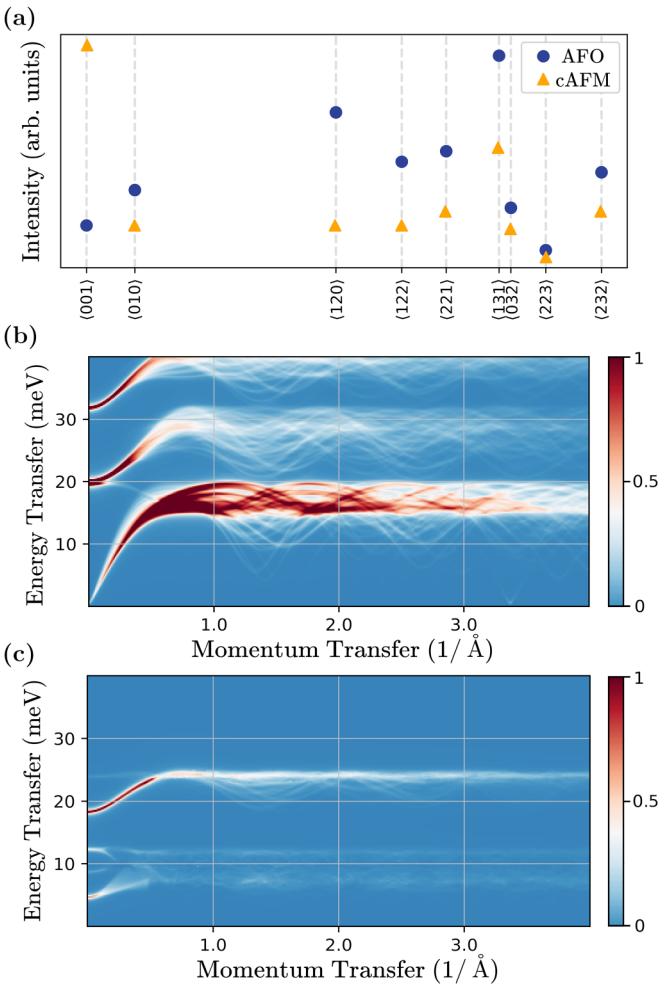

FIG. 3. Neutron scattering in SMRO. (a) Calculated intensities of the superstructural peaks $\langle hkl \rangle$ in polycrystalline SMRO in the octupolar AFO and cAFM phases. (b) Spherically averaged INS intensity in the AFO phase. (c) The same in the cAFM phase.

In Figs. 3(b) and 3(c) we display the corresponding inelastic neutron scattering (INS) intensities

$$\sum_{\alpha\beta}(\delta_{\alpha\beta} - \hat{q}_\alpha \hat{q}_\beta) \sum_{\mu\mu'} F^\alpha_\mu(\mathbf{q}) F^\beta_{\mu'}(\mathbf{q}) \text{Im}\chi_{\mu\mu'}(\mathbf{q}, E),$$

where $\chi_{\mu\mu'}(\mathbf{q}, E)$ is the multipolar dynamical susceptibility calculated with the random-phase approximation (RPA) [49]; we introduce $\mu \equiv KQ$ for brevity. The form factors were calculated including the covalency effect as described above, otherwise the approach is the same as in Ref. [45].

The calculated powder-averaged INS intensity in the AFO phase [Fig. 3(b)] features a bright "acoustic" branch, with a tiny gap of 0.6 meV hardly visible in Fig 3(b) but clearly resolved by zooming to the region of small q and E [36]. In addition, there are two "optical branches" of lower intensity.

Weak quasigapless dispersive branches are also observed at finite q values. The quasigapless modes stem from the almost exact U(1) symmetry of the projected pseudo-spin-1/2 Hamiltonian (2). The AFO INS spectrum is again drastically different from that of the cAFM phase [Fig. 3(c)]. The latter features a large gap and the higher-energy branch at about 25 meV exhibits the highest intensity.

Conclusions. We have derived the *ab initio* many-body effective Hamiltonian of SMRO, incorporating both electronic intersite exchange interactions and tetragonal/tilting lattice distortions. Our analysis reveals that intersite exchange interactions are significantly weaker than the induced $j_{\text{eff}} = 3/2$ splitting, leading to properties governed primarily by the ground state doublet.

By solving the effective Hamiltonian in the mean-field approximation, we uncover an antiferroic order of octupoles forming in SMRO at temperatures consistent with experimental observations. While this octupolar order was previously predicted at the model level [10], it has never been experimentally observed in a real material. The experimentally inferred collinear dipolar AFM order [25] can thus be interpreted as a "shadow play" with tiny dipole moments both entangled with the primary order octupolar parameters and hiding them.

To characterize this AFO phase and assess its stability, we explore the impact of structural parameters, finding that both tilting and tetragonal distortions play a crucial role in its stabilization with respect to a competing cAFM order of conventional dipole moments. We calculate experimentally observable signatures of the AFO order in elastic and inelastic neutron scattering, finding a quasigapless magnetic excitation spectrum and a strong enhancement of Bragg superstructural reflections at large q vectors. Overall, this study shows how hidden magnetic phases can emerge from Kramers' doublet ground states in distorted spin-orbit oxides, providing key insights into their primary driving mechanisms. Furthermore, it highlights a more complex physical scenario behind the previously proposed spin-glass phases in many tetragonally distorted $5d^1$ DPs. Revisiting these systems, in particular, isostructural Sr_2LiOsO_6 [22], could provide valuable new insights.

Acknowledgments. This research was funded in whole or in part by the Austrian Science Fund (FWF) 10.55776/J4698. For open access purposes, the author has applied a CC BY public copyright license to any author accepted manuscript version arising from this submission. D.F.M. thanks the computational facilities of the Vienna Scientific Cluster (VSC). L.V.P. is thankful to the CPHT computer team for support.

Data availability. The data that support the findings of this article are not publicly available. The data are available from the authors upon reasonable request.

[1] W. Witczak-Krempa, G. Chen, Y. B. Kim, and L Balents, Correlated quantum phenomena in the strong spin-orbit regime, Annu. Rev. Condens. Matter Phys. **5**, 57 (2014).

[2] T. Takayama, J. Chaloupka, A. Smerald, G. Khaliullin, and H. Takagi, Spin–orbit-entangled electronic phases in *4d* and *5d* transition-metal compounds, J. Phys. Soc. Jpn. **90**, 062001 (2021).

[3] P. Santini, S. Carretta, G. Amoretti, R. Caciuffo, N. Magnani, and G. H. Lander, Multipolar interactions in f-electron systems: The paradigm of actinide dioxides, Rev. Mod. Phys. **81**, 807 (2009).

[4] Y. Kuramoto, H. Kusunose, and A. Kiss, Multipole orders and fluctuations in strongly correlated electron systems, J. Phys. Soc. Jpn. **78**, 072001 (2009).

[5] H. Takagi, T. Takayama, G. Jackeli, G. Khaliullin, and S. E. Nagler, Concept and realization of Kitaev quantum spin liquids, Nat. Rev. Phys. **1**, 264 (2019).

[6] G. Jackeli and G. Khaliullin, Mott insulators in the strong spin-orbit coupling limit: From Heisenberg to a quantum compass and Kitaev models, Phys. Rev. Lett. **102**, 017205 (2009).

[7] D. D. Maharaj, G. Sala, M. B. Stone, E. Kermarrec, C. Ritter, F. Fauth, C. A. Marjerrison, J. E. Greedan, A. Paramekanti, and B. D. Gaulin, Octupolar versus Néel order in cubic $5d^2$ double perovskites, Phys. Rev. Lett. **124**, 087206 (2020).

[8] L Lu, M. Song, W. Liu, A. P. Reyes, P. Kuhns, H. O. Lee, I. R. Fisher, and V. F. Mitrović, Magnetism and local symmetry breaking in a Mott insulator with strong spin orbit interactions, Nat. Commun. **8**, 14407 (2017).

[9] D. Hirai, H. Sagayama, S. Gao, H. Ohsumi, G. Chen, T. Arima, and Z. Hiroi, Detection of multipolar orders in the spin-orbit-coupled $5d$ Mott insulator Ba_2MgReO_6, Phys. Rev. Res. **2**, 022063 (2020).

[10] G. Chen, R. Pereira, and L. Balents, Exotic phases induced by strong spin-orbit coupling in ordered double perovskites, Phys. Rev. B **82**, 174440 (2010).

[11] G. Chen and L. Balents, Spin-orbit coupling in d^2 ordered double perovskites, Phys. Rev. B **84**, 094420 (2011).

[12] C. Svoboda, W. Zhang, M. Randeria, and N. Trivedi, Orbital order drives magnetic order in $5d^1$ and $5d^2$ double perovskite Mott insulators, Phys. Rev. B **104**, 024437 (2021).

[13] D. Hirai and Z. Hiroi, Successive symmetry breaking in a $J_{\text{eff}} = 3/2$ quartet in the spin–orbit coupled insulator Ba_2MgReO_6, J. Phys. Soc. Jpn. **88**, 064712 (2019).

[14] N. Iwahara, V. Vieru, and L. F. Chibotaru, Spin-orbital-lattice entangled states in cubic d^1 double perovskites, Phys. Rev. B **98**, 075138 (2018).

[15] N. Iwahara and L. F. Chibotaru, Vibronic order and emergent magnetism in cubic d^1 double perovskites, Phys. Rev. B **107**, L220404 (2023).

[16] S. Agrestini, F. Borgatti, P. Florio, J. Frassineti, D. Fiore Mosca, Q. Faure, B. Detlefs, C. J. Sahle, S. Francoual, J. Choi, M. Garcia-Fernandez, K.-J. Zhou, V. F. Mitrović, P. M. Woodward, G. Ghiringhelli, C. Franchini, F. Boscherini, S. Sanna, and M. Moretti Sala, Origin of magnetism in a supposedly nonmagnetic osmium oxide, Phys. Rev. Lett. **133**, 066501 (2024).

[17] D. Fiore Mosca, C. Franchini, and L. V. Pourovskii, Interplay of superexchange and vibronic effects in the hidden order of Ba_2MgReO_6 from first principles, Phys. Rev. B **110**, L201101 (2024).

[18] D. Fiore Mosca, L. V. Pourovskii, B. H. Kim, P. Liu, S. Sanna, F. Boscherini, S. Khmelevskyi, and C. Franchini, Interplay between multipolar spin interactions, Jahn-teller effect, and electronic correlation in a $J_{\text{eff}} = \frac{3}{2}$ insulator, Phys. Rev. B **103**, 104401 (2021).

[19] J.-R. Soh, M. E. Merkel, L V. Pourovskii, I. Živković, O. Malanyuk, J. Pásztorová, S. Francoual, D. Hirai, A. Urru, D. Tolj, D. F. Mosca, O. V. Yazyev, N. A. Spaldin, C. Ederer, and H. M. Rønnow, Spectroscopic signatures and origin of hidden order in Ba_2MgReO_6, Nat. Commun. **15**, 10383 (2024).

[20] C. R. Wiebe, J. E. Greedan, P. P. Kyriakou, G. M. Luke, J. S. Gardner, A. Fukaya, I. M. Gat-Malureanu, P. L. Russo, A. T. Savici, and Y. J. Uemura, Frustration-driven spin freezing in the $S = \frac{1}{2}$ fcc perovskite Sr_2MgReO_6, Phys. Rev. B **68**, 134410 (2003).

[21] J. E. Greedan, S. Derakhshan, F. Ramezanipour, J. Siewenie, and T. Proffen, A search for disorder in the spin glass double perovskites Sr_2CaReO_6 and Sr_2MgReO_6 using neutron diffraction and neutron pair distribution function analysis, J. Phys.: Condens. Matter **23**, 164213 (2011).

[22] V. da Cruz Pinha Barbosa, J. Xiong, P. M. Tran, M. A. McGuire, J. Yan, M. T. Warren, R. V. Aguilar, W. Zhang, M. Randeria, N. Trivedi, D. Haskel, and P. M. Woodward, The impact of structural distortions on the magnetism of double perovskites containing $5d^1$ transition-metal ions, Chem. Mater. **34**, 1098 (2022).

[23] H. Kato, T. Okuda, Y. Okimoto, Y. Tomioka, K. Oikawa, T. Kamiyama, and Y. Tokura, Structural and electronic properties of the ordered double perovskites A_2MReO_6 (A = Sr,Ca; M = Mg,Sc,Cr,Mn,Fe,Co,Ni,Zn), Phys. Rev. B **69**, 184412 (2004).

[24] M. Retuerto, M. J. Martínez-Lope, M. García-Hernández, M. T. Fernández-Díaz, and J. A. Alonso, Crystal and magnetic structure of Sr_2MReO_6 (M = Ni, Co, Zn) double perovskites: A neutron diffraction study, Eur. J. Inorg. Chem. **2008**, 588 (2008).

[25] S. Gao, D. Hirai, H. Sagayama, H. Ohsumi, Z. Hiroi, and T.-H. Arima, Antiferromagnetic long-range order in the $5d^1$ double-perovskite Sr_2MgReO_6, Phys. Rev. B **101**, 220412 (2020).

[26] F. I. Frontini, G. H. J. Johnstone, N. Iwahara, P. Bhattacharyya, N. A. Bogdanov, L. Hozoi, M. H. Upton, D. M. Casa, D. Hirai, and Y.-J. Kim, Spin-orbit-lattice entangled state in A_2MgReO_6 (A = Ca, Sr, Ba) revealed by resonant inelastic x-ray scattering, Phys. Rev. Lett. **133**, 036501 (2024).

[27] R. Shiina, H. Shiba, and P. Thalmeier, Magnetic-field effects on quadrupolar ordering in a Γ_8-quartet system CeB_6, J. Phys. Soc. Jpn. **66**, 1741 (1997).

[28] P. Blaha, K. Schwarz, G. Madsen, D. Kvasnicka, J. Luitz, R. Laskowski, F. Tran, and L. D. Marks, *WIEN2k, An Augmented Plane Wave + Local Orbitals Program for Calculating Crystal Properties* (Karlheinz Schwarz, Techn. Universität Wien, Austria, 2018).

[29] A. Georges, G. Kotliar, W. Krauth, and M. J. Rozenberg, Dynamical mean-field theory of strongly correlated fermion systems and the limit of infinite dimensions, Rev. Mod. Phys. **68**, 13 (1996).

[30] V. I. Anisimov, A. I. Poteryaev, M. A. Korotin, A. O. Anokhin, and G. Kotliar, First-principles calculations of the electronic structure and spectra of strongly correlated systems: dynamical mean-field theory, J. Phys.: Condens. Matter **9**, 7359 (1997).

[31] A. I. Lichtenstein and M. I. Katsnelson, *Ab initio* calculations of quasiparticle band structure in correlated systems: LDA++ approach, Phys. Rev. B **57**, 6884 (1998).

[32] M. Aichhorn, L. V. Pourovskii, P. Seth, V. Vildosola, M. Zingl, O. E Peil, X. Deng, J. Mravlje, G. J Kraberger, C. Martins *et al.*, TRIQS/DFTTools: A TRIQS application for *ab initio* calculations of correlated materials, Comput. Phys. Commun. **204**, 200 (2016).

[33] J. Hubbard, Electron correlations in narrow energy bands, Proc. Roy. Soc. A **276**, 238 (1963).

[34] L. V. Pourovskii, Two-site fluctuations and multipolar intersite exchange interactions in strongly correlated systems, Phys. Rev. B **94**, 115117 (2016).

[35] L. V. Pourovskii and D. Fiore Mosca, MagInt, https://github.com/MagInteract/MagInt.

[36] See Supplemental Material at http://link.aps.org/supplemental/10.1103/tvp5-mpy9 for (i) detailed methods section (ii) intersite exchange interactions (iii) pseudo spin Hamiltonian projection (iv) tcf splitting as function of tilting and elongation (v) magnetic moment dependence as function of tcf (vi) excitation gap in the AFO phase and (vii) dependence of IEI on Coulomb U.

[37] W.-X. Qiu, J.-Y. Zou, A.-Y. Luo, Z.-H. Cui, Z.-D. Song, J.-H. Gao, Y.-L. Wang, and G. Xu, Efficient method for prediction of metastable or ground multipolar ordered states and its application in monolayer RuX_3 (X=Cl, I), Phys. Rev. Lett. **127**, 147202 (2021).

[38] Y. Wang, H. Weng, L. Fu, and X. Dai, Noncollinear magnetic structure and multipolar order in $Eu_2Ir_2O_7$, Phys. Rev. Lett. **119**, 187203 (2017).

[39] M. Rotter, Using *McPhase* to calculate magnetic phase diagrams of rare earth compounds, J. Magn. Magn. Mater. **272-276**, E481 (2004).

[40] A. Abragam and B. Bleaney, *Electron Paramagnetic Resonance of Transition Ions*, Oxford Classic Texts in the Physical Sciences (Oxford University Press, Oxford, 2012).

[41] K.-H. Ahn, K. Pajskr, K.-W. Lee, and J. Kuneš, Calculated *g*-factors of 5*d* double perovskites Ba_2NaOsO_6 and Ba_2YOsO_6, Phys. Rev. B **95**, 064416 (2017).

[42] M. Aichhorn, L. V. Pourovskii, V. Vildosola, M. Ferrero, O. Parcollet, T. Miyake, A. Georges, and S. Biermann, Dynamical mean-field theory within an augmented plane-wave framework: Assessing electronic correlations in the iron pnictide LaFeAsO, Phys. Rev. B **80**, 085101 (2009).

[43] A. Horvat, L. V. Pourovskii, M. Aichhorn, and J. Mravlje, Theoretical prediction of antiferromagnetism in layered perovskite Sr_2TcO_4, Phys. Rev. B **95**, 205115 (2017).

[44] L. V. Pourovskii and S. Khmelevskyi, Quadrupolar superexchange interactions, multipolar order, and magnetic phase transition in UO_2, Phys. Rev. B **99**, 094439 (2019).

[45] L. V. Pourovskii, D. Fiore Mosca, and C. Franchini, Ferro-octupolar order and low-energy excitations in d^2 double perovskites of osmium, Phys. Rev. Lett. **127**, 237201 (2021).

[46] We focus on low temperature and thus set the Debye-Weller factor to 1.

[47] R. Shiina, O. Sakai, and H. Shiba, Magnetic form factor of elastic neutron scattering expected for octupolar phases in $Ce_{1-x}La_xB_6$ and NpO_2, J. Phys. Soc. Jpn. **76**, 094702 (2007).

[48] S. W. Lovesey, *Theory of Neutron Scattering from Condensed Matter* (Clarendon Press, Oxford, 1984), Chap. 11.

[49] J. Jensen and A. R. Mackintosh, *Rare Earth Magnetism: Structures and Excitations* (Clarendon Press, Oxford, 1991).